Coupled Heat and Mass Transfer in Absorption of Water Vapor into LiBr-H_2O Solution Flowing on Finned Inclined Surfaces

Taebeom Seo*, Eunjun Cho

Department of Mechanical Engineering, Inha University, 253, Yonghyundong, Namgu, Inchon 402-751, Korea

The absorption characteristics of water vapor into a LiBr-H_2O solution flowing down on finned inclined surfaces are numerically investigated in order to study the absorbing performances of different surface shapes of finned tubes as an absorber element. A three-dimensional numerical model is developed. The momentum, energy, and diffusion equations are solved simultaneously using a finite difference method. In order to obtain the temperature and concentration distributions, the Runge-Kutta and the Successive over relaxation methods are used. The flat, circular, elliptic, and parabolic shapes of the tube surfaces are considered in order to find the optimal surface shapes for absorption. In addition, the effects of the fin intervals and Reynolds numbers are studied. The results show that the absorption mainly happens near the fin tip due to the temperature and concentration gradient, and the absorbing performance of the parabolic surface is better than those of the other surfaces.

Key Words : Absorption, LiBr, Absorber, Mass Transfer, Finned Tube

Nomenclature

A : Flow cross-sectional area of LiBr-H_2O solution [m^2]
a : Half of fin interval [m]
C : LiBr concentration
C_p : Specific heat of LiBr-H_2O solution [J/kg·K]
D : Diffusion coefficient of H_2O [m^2/s]
D_h : Hydraulic diameter [m]
h : Heat of absorption [J/kg]
l : Flow length of z direction [m]
n'' : Average mass flux of the absorbed water vapor at the interface per unit surface area projected on the x-z plane [kg/m^2s]
ΔP : Pressure difference between two fluids on the wall [N/m^2]
Pr : Prandtl number, ν/α
q'' : Heat flux accompanied with the phase change [J/m^2s]
q''_w : Average heat flux at the wall per unit surface area projected on the x-z plane [J/m^2s]
R : Radius of curvature of interface (free surface) [m]
Re : Reynolds number, $\bar{w}D_h/\nu$
Sc : Schmidt number, ν/D
T : Temperature [℃]
t : Effective thickness of LiBr-H_2O [m]
u, v, w : Velocities of the x, y, and z components [m/s]

Greek symbols

α : Thermal diffusivity of solution [m^2/s]
Γ : Mass flow of solution [kg/s]
ν : Kinematic viscosity of solution [m/s]
ϕ : Inclined angle [°]
θ : Contact angle [°]
ρ : Density of solution [kg/m^3]
γ : Coefficient of surface tension [N/m]

Subscripts

e : Interfacial

* Corresponding Author,
E-mail : seotb@inha.ac.kr
TEL : +82-32-860-7327; **FAX** : +82-32-868-1716
Department of Mechanical Engineering, Inha University, 253, Yonghyundong, Namgu, Inchon 402-751, Korea. (Manuscript **Received** November 25, 2003; **Revised** April 7, 2004)

b : Cross-sectional
w : Wall

1. Introduction

Since the use of CFC refrigerants is being restricted for conserving the environment, much research on absorption heat pumps and refrigerators has been carried out. Absorption, primarily, which is the most important process of the equipment, has been intensively investigated. Since the absorption phenomenon which occurs on complex surfaces between a number of tubes is so complicated, it is very difficult to analyze it numerically. Therefore, most of the research related to the absorption processes on complex surfaces is being done experimentally. For numerical investigations, only simplified geometry can be considered in order to find the solutions for problems with reasonable accuracy.

There were several typical numerical studies in which heat and mass transfer were considered simultaneously. Yih and Seagrave (1980) investigated liquid film, which had a linear temperature gradient along its depth but which neglected temperature variation in the flow direction. Grossman (1983) solved the energy and diffusion equations for the laminar liquid-film flow on an inclined flat plate assuming constant temperature of the adiabatic wall as the boundary condition. Lee et al. (1988) studied the heat and mass transfer of the LiBr-H_2O solution on a horizontal circular tube surface. Habib and Wood (1990) considered the simultaneous heat and mass transfer on vertical absorbers solving the momentum and energy equations for the vapor phase. Their two-phase concurrent flow was bounded by an isothermal wall on the liquid side and an adiabatic wall on the vapor side. These models can take care of steady-state solutions for smooth films. Uddholm and Setterwall (1988) presented the model considering both waviness and the coupled mass and heat transfer processes that occurred in falling films. Also, Wasden and Dukler (1990) performed numerical simulations to predict mass transfer to falling liquid films through wavy interfaces. Yang and Wood (1991) solved the conservation equations for the periodic wavy film. Vikas and Rerez-Blanco (1996) formulated two-dimensional governing equations for transient simultaneous heat and mass transfer in the film. These studies showed that wavy motion of falling liquid films increased heat and mass transfer significantly. The geometries adopted for these studies were two-dimensional and simple so that the models of these studies can be applicable to only non-finned cylinder or plate absorbers.

Many different complex three-dimensional surfaces have been developed as an absorber element to increase the heat and mass transfer rate. An experimental work was carried out to investigate the characteristics of water vapor absorption into LiBr-H_2O solution films falling on horizontal tubes by Hijikata at al.(1993). Isshiki and Ogawa (1987) introduced the CCS (constant curvature surface) tube, and the performances of the tubes were shown experimentally.

In order to optimally design an absorber, numerical investigation is very helpful. If the numerical estimation for heat and mass transfer is available we can significantly reduce the effort to get the design information from experiments. Based on the literature survey for the present study, however, numerical work for three-dimensional geometries hardly can be seen because of its difficulty.

In this study, heat and mass transfer of the LiBr-H_2O solution flowing between fins on inclined surfaces are numerically investigated in order to simulate absorption phenomenon on several different surfaces. In particular, the three-dimensional LiBr concentration distribution as well as the temperature distribution is investigated. Based on the calculated results, the performances of several geometries are estimated. In addition, the effects of the important design parameters, such as the surface shape and the fin interval, on the thermal performance of the tube element are analyzed.

2. Modelling

The schematic of the calculation domain for

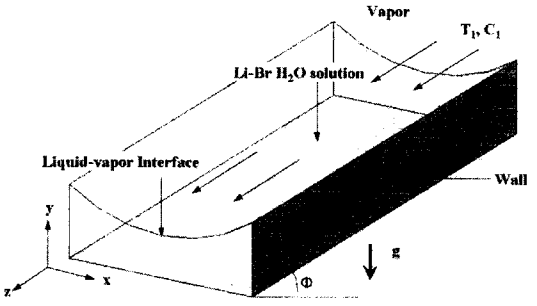

Fig. 1 Calculation domain

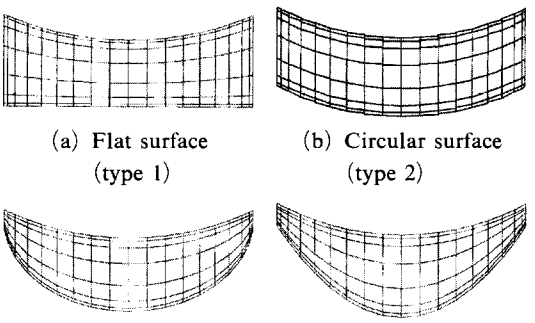

Fig. 2 Grid systems for each surfaces

the present study is shown in Fig. 1. Through the liquid-vapor interface the LiBr-H_2O solution flowing between fins on an inclined surface absorbs water vapor. The absorption of water vapor into a LiBr-H_2O solution, which is basically a phase change from vapor to liquid, is caused by partial pressure difference of H_2O between the LiBr-H_2O solution and the water vapor. When the phase change occurs at the liquid vapor interface, heat of absorption is generated so that heat as well as mass is transferred through the interface.

In order to simulate the absorption process on a finned inclined surface numerically, the following assumptions have been made:

(1) The properties of the LiBr-H_2O solution are independent of temperature and concentration.

(2) The mass of absorbed vapor is neglected so that the mass flow rate of the solution is constant.

(3) The flow between fins on an inclined surface is laminar.

(4) The flow is fully developed and its velocity has only a z-directional component from the entrance.

(5) Equilibrium of vapor pressure exists at the interface of the vapor and the solution.

(6) Surface tension is constant throughout the interface.

(7) The wall temperature including fins is kept constant and uniform.

2.1 Contact angle and surface tension

When two different fluids contact each other, surface tension is generated by the attraction of the molecules. If a fin interval is small enough to ignore the gravity, the interface shape of two fluids becomes circular (White, 1997). The surface tension is defined as the function of the pressure difference of the two fluids ΔP, and the interface radius R.

$$\Delta P=\frac{\gamma}{R} \tag{1}$$

where ΔP is assumed to be constant. Consequently, R becomes constant and the value can be determined from the contact angle and the fin interval. Fig. 2 shows the several different surface shapes of the solution flow. As mentioned before, the upper sides of the cross-sections are arcs of radius R. Therefore, the shapes shown in Fig. 2 can be identified by their lower sides, which are flat, circular, elliptic, and parabolic, respectively.

2.2 Velocity analysis

Based on the assumptions, the velocity has only the z-directional component and the others are zero. Also, it is assumed to be two-dimensional and fully developed. It is described as follows;

$$u,\ v=0,\ w=w(x,\ y) \tag{2}$$

$$\frac{\partial^2 w}{\partial x^2}+\frac{\partial^2 w}{\partial y^2}=\frac{1}{\mu}\left(\frac{\partial p}{\partial z}-\rho g \sin\phi\right) \tag{3}$$

Assuming that there is no pressure difference in the z-direction, $\partial p/\partial z$ becomes zero. In Fig. 3, three coordinate systems are shown; the x-y coordinate is for the cross-section, the x_1-y_1

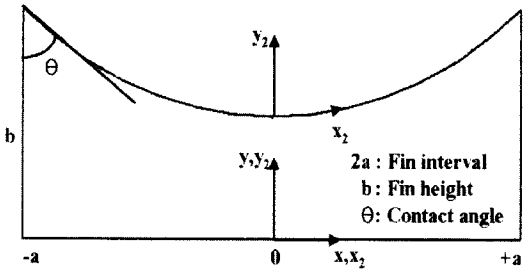

Fig. 3 Coordinate system for the x-y plane

coordinate is for the bottom surface, and the x_2-y_2 coordinate is for the interfacial surface. x_1 and x_2 are tangential to the bottom and interface at the center, respectively. Then, the following boundary conditions for the velocity can be used.

$$w=0 \text{ at } x=-a,\ a \text{ or } y_1=0 \tag{4}$$

$$\frac{\partial w}{\partial y_2}=0 \text{ at } y_2=0 \tag{5}$$

Eq. (4) means that the velocity at the wall is zero. Eq. (5) means that the velocity of the LiBr-H_2O solution is taken into account while the viscosity of water vapor is ignored.

2.3 Temperature and concentration analysis

In order to analyze temperature and concentration distributions, the steady-state energy and diffusion equations are solved.

$$w\frac{\partial T}{\partial z}=\frac{\nu}{\mathrm{Pr}}\left(\frac{\partial^2 T}{\partial x^2}+\frac{\partial^2 T}{\partial y^2}\right) \tag{6}$$

$$w\frac{\partial C}{\partial z}=\frac{\nu}{Sc}\left(\frac{\partial^2 C}{\partial x^2}+\frac{\partial^2 C}{\partial y^2}\right) \tag{7}$$

The boundary conditions for the equations are as follows:

$$T=T_w,\ \frac{\partial C}{\partial x}=0 \text{ at } x=-a,\ a \tag{8}$$

$$T=T_w,\ \frac{\partial C}{\partial y_1}=0 \text{ at } y_1=0 \tag{9}$$

The boundary conditions (Eq. (8)-(9)) mean that the wall temperature is uniform and the mass cannot be transferred through the wall. Both the temperature and the concentration at the interface are unknown. However, if the pressure at the interface in equilibrium is constant, the temperature can be represented as the function of concentration as follows:

$$T_e=f(C_e) \text{ at } y_2=0 \tag{10}$$

The heat of absorption at the interface is the function of the amount of the absorbed mass when the phase change occurs.

$$q_e''=h\cdot n'' \tag{11}$$

If the concentration change of the LiBr-H_2O solution is small at constant pressure, Eq. (10) can be linear as follows (Mcneely, 1985):

$$T_e=B_1C_e+B_2 \tag{12}$$

Unknown interfacial temperature and concentration is determined from Eq. (11) and (12).

2.4 Numerical analysis

x-y grids which are generated by the algebraic grid generation method are 28×31. The explicit scheme is used so that the interval of z grids must be very small to have a converged solution. To satisfy the convergent criterion, the number of z grids is over 10^7. It takes about 24 hours on a 450 MHz Pentium II CPU. To make sure that stable solution is obtained, the grid sensitivity is checked. Although the dense grid system is used so that the calculation time on the same machine becomes about 5-7 times longer, the difference between the two solutions is less than 2% at most.

The SOR (Successive Over Relaxation) method is used to solve Eq. (3) for the velocity. In order to solve temperature and concentration, the Runge-Kutta and finite difference method are used except for the interfacial temperature and concentration. The interfacial temperature and concentration are solved by the SOR method using Eq. (11) and (12). In Fig. 4 the flow chart of the present calculation is given to show the calculation procedure.

There are discontinuities in the temperature and concentration fields between the interface and the entrance surface. To numerically avoid

this problem, the solutions within 10^{-12} m from the entrance are calculated using the entrance temperature and concentration as the interfacial data. Table 1 shows the calculating conditions and properties used for the present study. It is very difficult to know the contact angle of the LiBr-H_2O solution on the tube element surface because there are many uncertainties to fix the value. Thus, the contact angle is always assumed to be 60°.

Table 1 Calculating conditions and properties

l	0.03 m	k	0.487 W/m·K
T_i	50℃	h	2.721×10^6 J/kg
C_i	0.6	D	1.6×10^{-9} m²/s
T_w	30℃	ν	3.0×10^{-6} m²/s
P_e	9.2 mmHg	ϕ	45°
ρ	1700 kg/m³	θ	60°
C_p	1570 J/kg·K	Pr	21.43
g	9.807 m/s²	Sc	1875

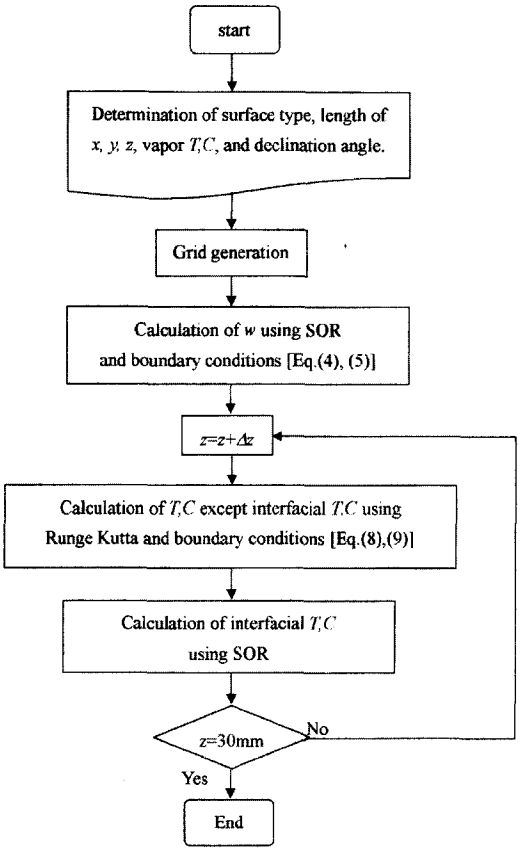

Fig. 4 Flow chart of the calculation

3. Results and Discussion

Table 2 shows the flow conditions and the results of mass flow rates Γ and mean velocities for each surface. After setting the Reynolds, Prandtl, and Schmidt numbers equal, we can compare the flow and absorption characteristics $\bar{w}$ for each surface. Generally, Re on a tube surface of an absorber is smaller than 100 so that Re of 70 is selected for the present calculation. D_h and $\bar{w}$ are decided by iterative calculation for each surface until Re becomes 70. For the elliptic and parabolic shapes, it is assumed that the fin heights are 20% of the distances from the bottom of the surface and the fin tip. As shown in the table, the differences of $\bar{w}$'s are small, but those for Γ are relatively large. Γ of type 1 is the largest. It means that a difference of effective thickness t of flow exists, and it is defined as Eq. (13).

$$\Gamma=\rho\bar{w}A\approx\rho\bar{w}(t\cdot 2a) \tag{13}$$

It can be obtained from Eq. (13) that t's of type 1, 2, 3, and 4 are 6.25×10^{-4}, 5.75×10^{-4}, 5.35×10^{-4}, 5.28×10^{-4}, respectively. The reason why the effective thickness is different is because of the difference of the viscous effect in the channel. The thickness of type 1 is the thickest and that of type 4 is the thinnest. Looking at Fig. 5 and Fig. 6, we can find that the interface temperature and concentration become lower if the effective thickness becomes thinner. In particular, the thickness of flow near the fin tip should be thin like type 4 rather than in the middle between the fins. Even though the effective thickness of flow is thin, the absorbing performance can be bad if the thickness

Table 2 Flow conditions and results

	Type 1	Type 2	Type 3	Type 4
Re	70	70	70	70
Pr	21.43	21.43	21.43	21.43
Sc	1875	1875	1875	1875
Γ[kg/s]	3.2E-4	2.9E-4	2.7E-4	2.7E-4
$\bar{w}$[m/s]	0.1506	0.1484	0.1485	0.1503

of flow near the fin is thick. This fact has been checked using the numerical model developed in the study.

Figure 5 shows the mean temperatures of the interface and the cross-section for Re at 70 with a fin interval of 2 mm. The interface mean temperature T_e along the z-direction is linearly reduced except for the entrance vicinity. On the other hand, the cross-sectional mean temperature T_b rapidly decreases near the entrance, and then, gradually decreases along the z-direction.

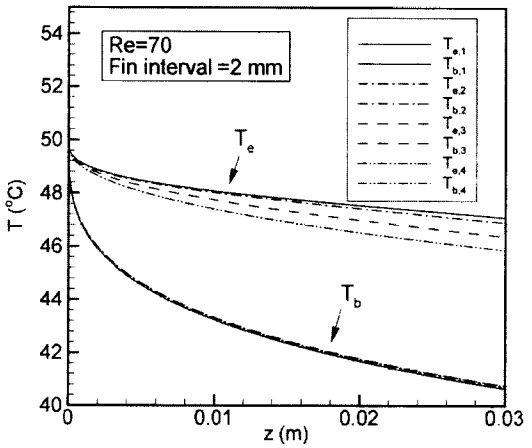

Fig. 5 Variation of the mean temperatures of the interface and the flow cross-section along the z-direction

The decreasing rate of T_b is much greater than that of T_e. The differences of T_b's between the surfaces are small. Since T_b is not an important parameter for the water vapor absorption into LiBr-H_2O solution through the interface, its small differences do not have a significant physical meaning. The reason why we make the temperature of the solution low is to make the interfacial temperature low, rather than the cross-sectional mean temperature. T_e of type 4 is lower than those of other types. It means that the heat transfer rate of type 4 at the interface is the greatest.

In Fig. 6, the mean LiBr concentration of the interfaces and of the cross-sections for the different surfaces are shown as Re of 70 with a fin interval of 2 mm. The mean LiBr concentrations at the cross-section C_b are almost the same and do not vary significantly along the z-direction. On the other hand, the mean LiBr concentrations at interface C_e are different from each other and they decrease gradually along the z-direction : C_e of type 4 is the lowest among them. The lowest LiBr concentration means the highest H_2O concentration. Therefore, the amount of absorbed water vapor of type 4 is the greatest for the given operating conditions.

The average heat flux q''_w is shown in Fig. 7 with a Re of 70 and a fin interval of 2 mm. For q''_w evaluation, the projected area of the surface

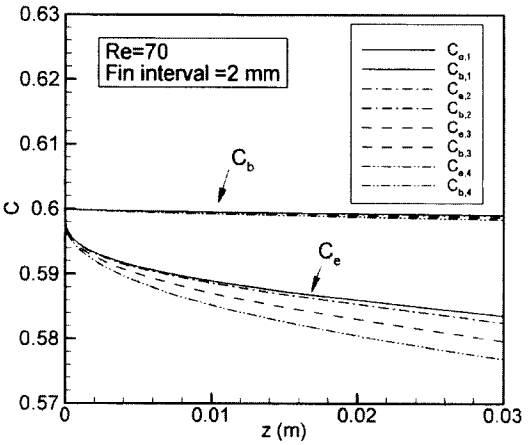

Fig. 6 Variation of the mean concentrations of the interface and the flow cross-section along the z-direction

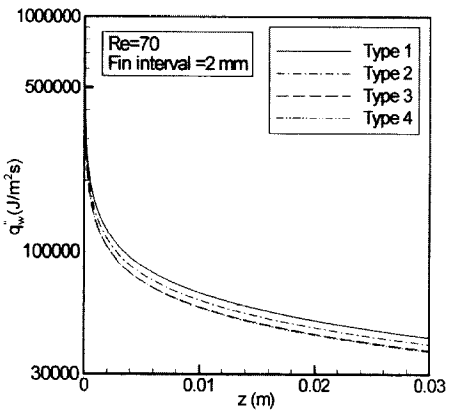

Fig. 7 Variation of the average heat fluxes based on the surface area projected on the x-z plane along the z-direction

on the x-z plane is taken into account because it is easy to compare the results with each other. In addition, it is not important to obtain the heat and mass fluxes through all the heat and mass transfer surfaces, but to calculate those with respect to the surface area between the two consecutive fins. Thus, exact q''_w can be calculated as follows:

$$q''_w=\frac{1}{2a}\left(\sum_{i=1}^{n}k\frac{\partial T_i}{\partial y_1}\Delta x_{1,i}|_{y_1=0}+\sum_{i=1}^{n}k\frac{\partial T_i}{\partial x}\Delta(y_2-y_1)_i|_{x=-a,a}\right) \quad (14)$$

In Fig. 7, q''_w decreases rapidly near the entrance and then gradually decreases along the z-direction, which is similar to the typical heat transfer trend of the channel flow near the entrance. q''_w of type 1 at the z=30 mm is about 10 % greater than type 3 and 4, but the perimeter of the heat transfer area of type 1 is about 20 % longer than those of type 3 and 4. Therefore, the heat transfer rates through all the surfaces of type 3 and 4 are greater than those of type 1. The perimeter and q''_w of type 3 and 4 are almost the same. However, it is shown in Fig. 8 that the amount of water vapor absorption of type 4 is larger than that of type 3. As mentioned above, heat transfer through the interface is important for the purpose of absorption. Therefore, q''_w, which means heat transfer on the tube surface, is not necessarily an important parameter for water vapor absorption.

Fig. 8 shows the average mass flux of the absorbed vapor at the interface with respect to the interfacial area projected on the x-z plane, n'', with a Re of 70 and a fin interval of 2 mm. Thus, n'' can be calculated as follows:

$$n''=\frac{1}{2a}\sum_{i=1}^{n}\rho D\frac{\partial C_i}{\partial y_2}\Delta x_{2,i}|_{y_2=0} \quad (15)$$

n'' gradually increases along the z-direction except for the entrance vicinity. The steep temperature gradient between the fin tip and the solution occurs near the entrance. Consequently, the temperature of the solution around the fin tip decreases so that the water vapor is absorbed through this particular area. While the solution flows down, the temperature gradient is gradually developed so that the interface area in which the solution temperature is lower than the inlet temperature expands. Therefore, the amount of absorbed water vapor increases along the z-direction. n'' of type 4 at the z=30 mm is about 37 % greater than that of type 1. This means that type 4, which is parabolic, makes heat transfer on the interface efficient and the mass transfer rate of the water vapor into the solution increases.

In Fig. 9, the average mass fluxes of the absorbed vapor at the interface with respect to the interfacial area projected on the x-z plane n''_{avg} for the different surfaces and the fin intervals are shown. It is found from Fig. 9 that the absorption performance of type 4 is the best. If

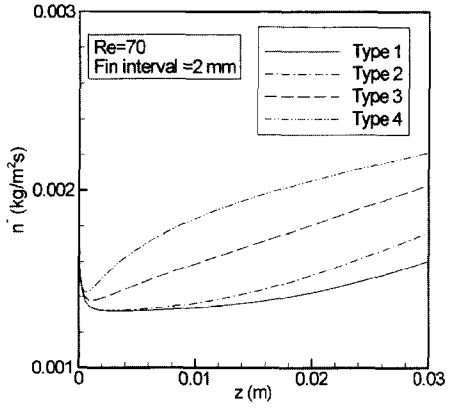

Fig. 8 Variation of the mass fluxes based on the interface area projected on the x-z plane along the z-direction

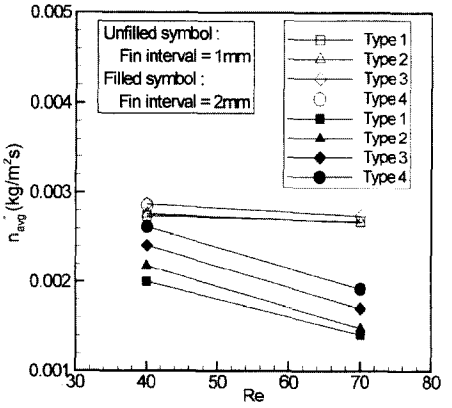

Fig. 9 Average mass fluxes based on the surface area projected on the x-z plane for different surfaces and fin interval

Re is low and the fin interval becomes narrow, n''_{avg} increases. When the fin interval is 1 mm, the differences of the amount of the absorbed water vapor between the different surfaces are not big unlike the fin interval of 2 mm. When the fin interval is 1 mm and the Re is 70, it is impossible to obtain the solution for type 4. Although the fin height is assumed to be high, overflowing of the solution on the fins inevitably occurs. Once it happens, the effect of the surface tension disappears.

In order to summarize the calculated results, all the data for type 3 are given in Table 3 and 4. In Table 3, the average heat and mass fluxes for different Reynolds numbers and fin heights are shown at different axial locations. Also, the same data for different fin intervals and fin heights are summarized in Table 4.

The contours of the LiBr concentration for the cross-sections of type 1 and type 4 are represented in Fig. 10 for the Re of 70 and the fin interval of 2 mm at $z=30$ mm. It is found that the absorbing zones exist near the fin tips. Based on the results, the role of the fin is not only to increase the interface, but also to make the steep concentration gradient so that the solution absorbs the vapor as much as possible. If the flow length z is not long enough, the water vapor may be absorbed only near the fin tips. Also, it is known from Fig. 10 that the amount of the

Table 3 Average heat and mass fluxes at the wall projected on x-z plane for type 3 for different Reynolds numbers

Declination angle=45°, Fin interval=1 mm				
Re	y (mm) Fin height	z (mm)	$q''_{w,avg}$ (kW/m²)	n''_{avg} (kg/m²s) ($\times 10^3$)
20	6.295	10	66.76	3.187
		20	47.13	3. 614
		30	37.66	3.883
30	8.065	10	84.03	2.825
		20	60.36	3.013
		30	48.80	3.175
40	1.028	10	102.2	2.685
		20	74.44	2.788
		30	60.82	2.870
50	1.340	10	132.9	2.632
		20	97.33	2.704
		30	79.86	2.758
60	1.866	10	188.9	2.616
		20	138.5	2.675
		30	113.7	2.718
70	3.115	10	312.3	2.635
		20	228.9	2.699
		30	187.8	2.744
80	20.30	10	2142	2.808
		20	1548	2.977
		30	1258	3.095

Table 4 Average heat and mass fluxes at the wall projected on x-z plane for type 3 for different fin intervals

Declination angle=45°, Re=70				
x (mm) Fin interval	y (mm) Fin height	z (mm)	$q''_{w,avg}$ (kW/m²)	n''_{avg} (kg/m²s) ($\times 10^3$)
0.96	10.000	10	1072	2.892
		20	768.3	3.043
		30	619.2	3.146
1.00	3.115	10	312.3	2.635
		20	228.9	2.699
		30	187.5	2.744
1.20	1.246	10	106.3	2.186
		20	80.13	2.238
		30	67.40	2.280
1.40	1.013	10	84.07	1.925
		20	63.61	1.991
		30	53.70	2.049
1.60	0.931	10	77.76	1.737
		20	59.07	1.819
		30	50.02	1.894
1.80	0.898	10	82.34	1.593
		20	62.80	1.690
		30	53.32	1.783
2.00	0.886	10	77.83	1.478
		20	59.78	1.590
		30	50.96	1.703

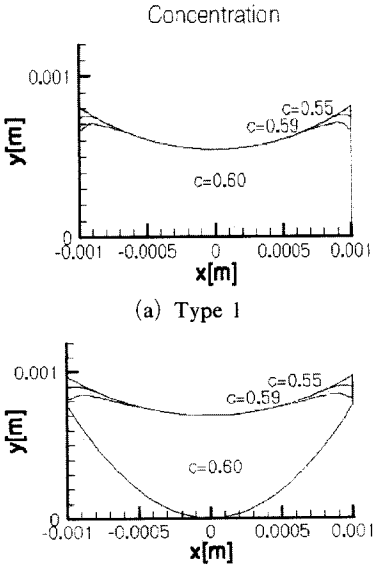

Fig. 10 Contours of LiBr concentration at $z=30$ mm (Re=70)

absorbed water vapor of type 4 is greater than that of type 1, even though the difference is not significant on the figure.

4. Conclusions

The characteristics of heat and mass transfer of the LiBr-H_2O solution flowing between fins on the inclined surface were numerically investigated. In particular, different shapes of surfaces were considered and the absorbing performance depending upon the surface shapes was carefully investigated. Based on the results, it was found that absorption occurred mainly near the fin tips because the temperature and concentration gradients were generated. Therefore, if we make the actual absorbing area like the near fin tips large, absorbing performance would increase. In order to increase the actual absorbing area, the effective thickness of flow should be thin. In particular, the thickness of flow near the fin must be thin rather than in the middle between the fins. Based on this argument, surface type 4, which was parabolic, was the best for these operating conditions among the surfaces considered in the study as shown from the results.

References

Grossman, G., 1983, "Simultaneous heat and mass transfer in film absorption under laminar flow," *International Journal of Heat and Mass Transfer*, 26, 357.

Habib, H. M. and Wood, B. D., 1990, "Simultaneous heat and mass transfer for a falling film absorber," *the Proceedings of the 12th annual ASME International Solar Energy Conference*, 61.

Hijikata, K., Lee, S. K. and Nagasaki, T., 1993, "Water vapor absorption enhancement in LiBr/H_2O films falling on horizontal tubes," *Journal of the Japan Society of Mechanical Engineers*, 58, 243~248.

Isshiki, N. and Ogawa, K., 1987, "New thermodynamic cycles for utilization of low temperature difference energy sources and new heating surface called CCS," *JSME 25th Power-Energy Utilization Symposium*, Tokyo, 63.

Lee, K. S., Seo, S. C., Kim, Y. I. and Park, D. K., 1988, "Coupled heat and mass transfer during the absorption of water vapor into LiBr-H_2O liquid solution flowing down the outside of the horizontal cylinder," *Korean Journal of Air-Conditioning and Refrigeration Engineering*, 17, 140.

Mcneely, L. A., 1985, "Thermodynamic properties of aqueous solutions of lithium bromide," *ASHRAE Trans*, 413.

Uddholm, H. and Setterwall, F., 1988, "Model for dimensioning a falling film absorber in an absorption heat pump," *International Journal of Refrigeration*, 11, 41.

Vikas, P. and Parez-Blanco, H., 1996, "A study of absorption enhancement by wavy film flows," *International Journal of Heat and Fluid Flow*, 17, 71.

Wasden, F. K. and Dukler, A. E., 1990, "A numerical study of mass transfer in free falling wavy films," *AIChE Journal*, 36, 1379.

White, F. M., 1997, *Fluid Mechanics, 3rd ed.*, McGraw Hill international editions, 26.

Yang, Ru. and Wood, Byard. D., 1991, "A numerical solution of the wavy motion on a

falling liquid film," *The Canadian Journal of Chemical Engineering*, 69, 723.

Yih, S. M. and Seagrave, R. C., 1980, "Mass transfer in laminar falling liquid film with accompanying heat and interfacial shear," *International Journal of Heat and Mass Transfer*, 23, 749.